and isolated by crystallization from CH_3CN in 36% yield.[15] The tertiary proton and carbon resonances for the *i*-Pr groups on the aryl imide ligand are broadened at room temperature in purple **5**, presumably due to hindered rotation about the (*i*-Pr)-C_6H_3 bonds. The ^1H NMR signal sharpens into a septet at 40 °C while no other line-shape changes are observed.

Reactions of **2a** with alcohols depend on the nature of the substituent. Complex **2a** did not react with *t*-BuOH at room temperature, but the deep red CymOs(O-*t*-Bu)$_2$ (**6**) could be prepared by treatment of **1a** with 2 equiv of *t*-BuOK in THF.[16] Complex **6** was characterized spectroscopically, but repeated attempts to isolate it in analytically pure form have not succeeded. The bis(*tert*-butoxide) **6** was converted to the monomeric imido complex **2a** upon addition of *t*-BuNH$_2$, demonstrating that $\Delta G° > 0$ for the **2a** + *t*-BuOH reaction. In contrast to these observations with *t*-BuOH, addition of pinacol ($HOC(CH_3)_2C(CH_3)_2OH$) to **2a** in pentane led to >98% yield (by ^1H NMR integration against an internal standard) of the red pinacolate CymOs[$OC(CH_3)_2C(CH_3)_2O$] (**7**).[17] The compound was isolated in 34% yield on a preparative-scale reaction after purification by crystallization from diethyl ether. Electron-impact mass spectroscopy of complex **7** shows the monomeric molecular ion at *m/e* 442.

Although **2a** does not react with *t*-BuOH, addition of *t*-BuSH to **2a** in toluene gave the violet CymOs(S-*t*-Bu)$_2$ (**8**) in 95% yield.[18] The bis(*tert*-butoxide) **6** was also converted to **8** upon addition of 2 equiv of *t*-BuSH. In each case, *t*-BuNH$_2$ or *t*-BuOH was observed by ^1H NMR spectrometry as a byproduct of the transformation. Variable-temperature ^1H and $^{13}C\{^1H\}$ NMR studies show no line-shape changes from 25 to -80 °C.[19] The thiolate **8** is monomeric in the mass spectrum, showing $[M]^+$ at *m/e* 504, but no peak at higher mass. Attempts to prepare CymOs(NH-*t*-Bu)$_2$ for direct comparison with **6**, **7**, and **8** by addition of limited amounts (2 equiv) of LiNH-*t*-Bu to **1a** led only to a mixture of **1a** and **2a**.

Monomeric compounds **2a** and **2b** provide additional evidence for the enhanced reactivity of late transition metal imides. These complexes have opened up an opportunity to study Os-X bonds (X = N, O, S) in low-valent osmium compounds and to prepare unusual late transition metal heteroatom bonded complexes. Experiments aimed at exploring these possibilities are under way.

Acknowledgment. We are grateful for financial support for this work from the National Institutes of Health (Grant No. GM-25459) and to Degussa AG for a loan of $OsCl_3 \cdot 3H_2O$. We thank James Gilchrist and Prof. David Collum for providing us with the details of their $H_2{}^{15}N$-*t*-Bu preparation.

Supplementary Material Available: Spectroscopic (**2-8**) and analytical data (**2a,b**, **3**, **4**, **7**, and **8**) and details of the structure determination for complex **2b**, including experimental description and ORTEP drawing showing full atomic numbering, tables of crystal and data collection parameters, positional parameters and their estimated standard deviations, and intermolecular distances and angles (11 pages); tables of observed and calculated structure factors for **2b** (13 pages). This material is included with the archival edition of the journal, available in many libraries. Alternatively, ordering information is given on any current masthead page.

(16) For a review of monomeric late-metal alkoxides, see: (a) Bryndza, H. E.; Tam, W. *Chem. Rev.* **1988**, 1163 and references therein. Also see: (b) Hartwig, J. F.; Andersen, R. A.; Bergman, R. G. *J. Organomet. Chem.* **1990**, *394*, 417. (c) Komiya, S.; Tane-Ichi, S.; Yamamoto, A.; Yamamoto, T. *Bull. Chem. Soc. Jpn.* **1980**, *53*, 673.

(17) For a review including some metallapinacols, see: (a) Kahn, B. E.; Rieke, R. D. *Chem. Rev.* **1988**, *88*, 733. Other monomeric metallapinacols have been prepared in our lab and other labs: (b) McCallum, J. S.; Glueck, D. S.; Bergman, R. G. unpublished results. (c) Andrews, M. A.; Gould, G. L. *Organometallics* **1991**, *10*, 387.

(18) For saturated late transition metal bis(thiolates), see: Klein, D. P.; Kloster, G. M.; Bergman, R. G. *J. Am. Chem. Soc.* **1990**, *112*, 2022 and references therein.

(19) A dimer for **8** would be expected to show two *tert*-butyl resonances (terminal and bridging).

A Neutral, Water-Soluble, α-Helical Peptide: The Effect of Ionic Strength on the Helix-Coil Equilibrium

J. Martin Scholtz,† Eunice J. York,‡ John M. Stewart,‡ and Robert L. Baldwin*,†

Department of Biochemistry
Stanford University School of Medicine
Stanford, California 94305
Department of Biochemistry
University of Colorado Health Science Center
Denver, Colorado 80262

Received January 14, 1991

Short, alanine-based peptides that are made water-soluble by insertion either of glutamic acid and lysine residues[1] or of lysine alone[2] can adopt an α-helical structure in aqueous solution. A recent calorimetric study[3] suggests that the α-helical polypeptide backbone itself is responsible for the stability of the helix in water. These and other peptides are being used to study the helix propensities of amino acids by substitution experiments.[4-7] Introduction of an uncharged reference peptide could be a significant advance, particularly for determining helix propensities of charged amino acids. We report the synthesis and characterization of such an uncharged helix-forming peptide that contains naturally occurring amino acids.[8] The 16-residue peptide contains three blocks of the simple repeat[11] AAQAA; four alanine residues separate successive glutamine residues. The peptide sequence is Ac-$(AAQAA)_3Y(NH_2)$. The single tyrosine residue allows accurate measurement of peptide concentration by tyrosine absorbance.[2] The acetyl and amide blocking groups eliminate the charges on α-NH_3^+ and α-COO^- groups, respectively. Insertion of three glutamine residues provides water solubility; the poly-L-alanine sequence is not soluble.

The circular dichroism (CD) spectrum of the peptide (Figure 1) shows the two minima at 222 and 208 nm and the maximum close to 190 nm that are characteristic of mixtures of α-helix and random coil structures,[12] and the helix unfolds with increasing temperature (Figure 1), like other alanine-based peptides.[1-3] The value of $-[\theta]_{222}$ at 0 °C in 0.1 M NaCl (16 500 deg cm^2 dmol^{-1}) is somewhat lower than the values reported[2] (~22 000) for some different 16-residue, alanine-based peptides that contain three lysine residues. Thermal-unfolding curves are coincident over a broad range of peptide concentration (from 8.5 to 119 μM), which shows that helical stability is not concentration dependent and therefore the helix is probably monomeric. An earlier study of

* To whom all correspondence should be addressed.
† Stanford University School of Medicine.
‡ University of Colorado Health Science Center.

(1) Marqusee, S.; Baldwin, R. L. *Proc. Natl. Acad. Sci. U.S.A.* **1987**, *84*, 8898.

(2) Marqusee, S.; Robbins, V. H.; Baldwin, R. L. *Proc. Natl. Acad. Sci. U.S.A.* **1989**, *86*, 5286.

(3) Scholtz, J. M.; Marqusee, S.; Baldwin, R. L.; York, E. J.; Stewart, J. M.; Santoro, M.; Bolen, D. W. *Proc. Natl. Acad. Sci. U.S.A.* **1991**, *88*, 2854.

(4) Padmanabhan, S.; Marqusee, S.; Ridgeway, T.; Laue, T. M.; Baldwin, R. L. *Nature* **1990**, *344*, 268.

(5) Merutka, G.; Lipton, W.; Shalongo, W.; Park, S.-H.; Stellwagen, E. *Biochemistry* **1990**, *29*, 7511.

(6) Lyu, P. C.; Liff, M. I.; Marky, L. A.; Kallenbach, N. R. *Science* **1990**, *250*, 669.

(7) O'Neil, K. T.; DeGrado, W. F. *Science* **1990**, *250*, 646.

(8) Peptide synthesis was performed by standard solid-phase methods.[9,10] Peptide purification was performed by using HLPC as described.[3] Peptide purity was determined by amino acid analysis and FABMS (calculated MW 1458.73, found $(M + H)^+$ 1459.46, $(M + Na)^+$ 1481.18). Coincidence of the electrophoretic mobilities of the peptide at pH 5.0 and 2.8 was used to confirm that the glutamine side chains had not hydrolyzed to glutamic acid during the synthesis or purification of the peptide.

(9) Stewart, J. M.; Young, J. D. *Solid Phase Peptide Synthesis*, 2nd ed.; Pierce Chemical Co.: Rockford, IL, 1964.

(10) Hudson, D. *J. Org. Chem.* **1988**, *53*, 167.

(11) Abbreviations used: A, L-alanine; Q, L-glutamine; Y, L-tyrosine; CD, circular dichroism.

(12) Holzwarth, G.; Doty, P. *J. Am. Chem. Soc.* **1965**, *87*, 218.

0002-7863/91/1513-5102$02.50/0

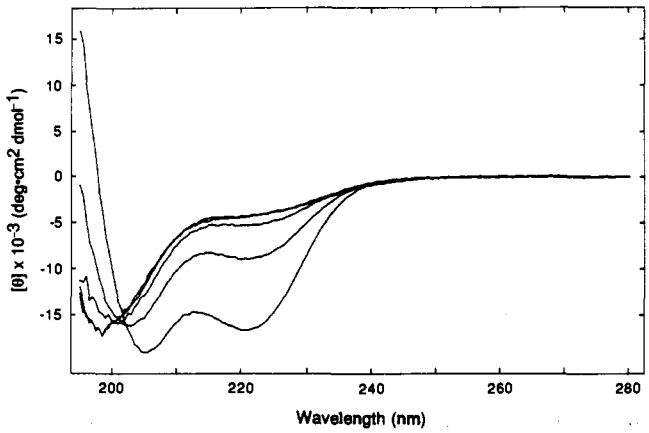

Figure 1. Circular dichroism (CD) spectra of $Ac(AAQAA)_3Y(NH_2)$ recorded at 0, 20, 40, 60, and 80 °C with an Aviv 60DS spectropolarimeter as described.[1-4] At 222 nm, the bottom curve represents the spectrum at 0 °C and the top curve at 80 °C. The peptide concentration was 24.2 μM in 1 mM KH_2PO_4 containing 0.1 M KF at pH 7.0.

lysine-containing, alanine-based peptides[4] showed that this is a reliable test by comparison with measurements of molecular weight by sedimentation equilibrium.

Availability of a completely neutral helix allows us to test a prediction based on the 1943 theory of Kirkwood[13] for the thermodynamic interaction between a dipolar ion and an electrolyte. The prediction is that increasing ionic strength should stabilize the helix by shifting the equilibrium between the α-helix (which should have a large dipole moment[14,15]) and the random coil (which has a small dipole moment since the peptide dipoles are oriented almost randomly). Like the Debye–Hückel theory,[16] Kirkwood's theory is a limiting law, applicable at low values of the ionic strength.[17] Figure 2A shows that there is an increase in α-helix content with ionic strength, at low ionic strength, for each of three salts that are either helix-stabilizing (Na_2SO_4) or -destabilizing ($CaCl_2$, NaCl) at high ionic strength. In Figure 2B, $\Delta G°$ for helix formation has been calculated from α-helix to random coil theory.[18,19] The lines at high electrolyte concentration show the linear behavior expected for the effect of a Hofmeister series salt on the logarithm of the activity coefficient of a nonpolar molecule.[20] Figure 2C compares the change in $\Delta G°$ with ionic strength for the three salts after subtracting the Hofmeister effect. An identical linear change with ionic strength is found for the three different salts, as expected from Kirkwood's theory.

The magnitude of the dipole moment of the α-helix, estimated from the slope of the line in Figure 2C using Kirkwood's model,[13,17] is 51 D. This gives a per residue dipole moment of 3.2 D, which is identical with the residue dipole moment (3.2–3.4 D) measured for the γ-benzyl ester of poly-L-glutamate in various organic solvents.[14] The agreement between these values may be coincidental; a detailed investigation of Kirkwood's theory, for the specific case of a neutral α-helix, may show that the electrolyte ions interact with partial charges on the NH and CO groups that are not H-bonded at either end of the helix, rather than with the α-helix macrodipole itself.[21]

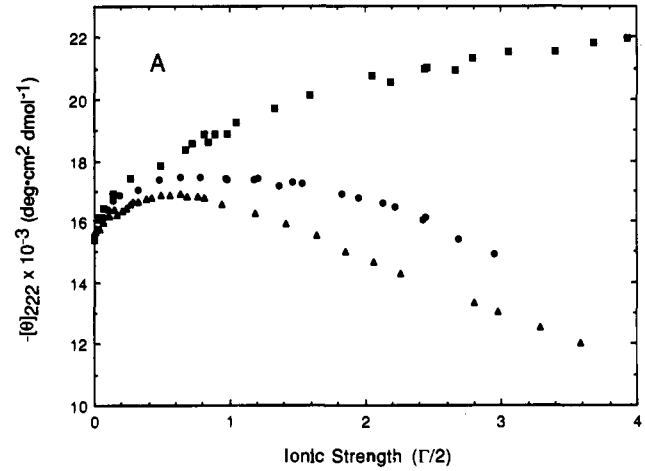

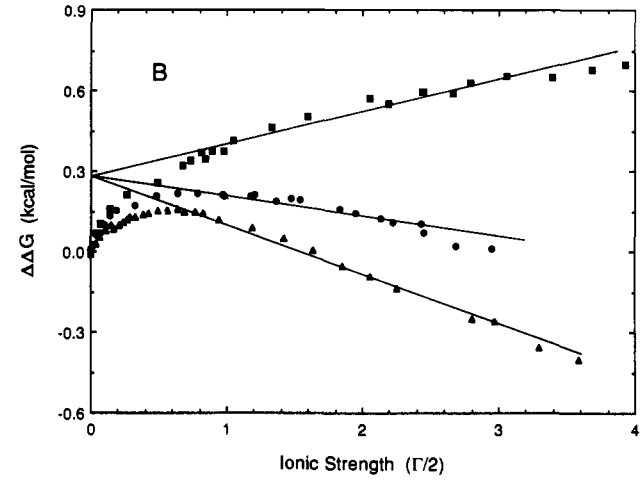

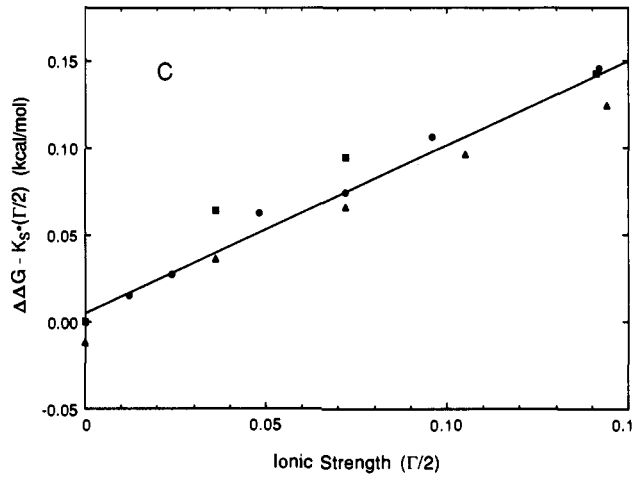

Figure 2. (A) Helical content of the peptide as a function of ionic strength for each of the three salts: Na_2SO_4 (■), NaCl (●), and $CaCl_2$ (▲). The helical content was determined by CD at 0 °C in 1.0 mM NaH_2PO_4 at pH 7.0. (B) Changes in free energy ($\Delta\Delta G°$) for helix stability[19] as a function of ionic strength for each of the three salts: $\Delta\Delta G° = \Delta G°(\Gamma/2=0) - \Delta G°(\Gamma/2>0)$. (C) Changes in free energy for helix stability after subtraction of the specific Hofmeister effect ($K_s•(\Gamma/2)$) for each of the three salts. The limiting slope can be used to calculate the dipole moment of the dipolar ion using Kirkwood's model (see text).[13]

(13) Kirkwood, J. G. In *Proteins, Amino Acids and Peptides*; Cohn, E. J., Edsall, J. T., Eds.; Reinhold Publishing: New York, 1943; p 275.
(14) Wada, A. *Adv. Biophys.* **1976**, *9*, 1.
(15) Hol, W. G. J. *Prog. Biophys. Mol. Biol.* **1985**, *45*, 149.
(16) Debye, P.; Hückel, E. *Phys. Z.* **1923**, *24*, 185.
(17) Kirkwood gives equations for three different cases, depending chiefly on the relative dimensions of the molecule, represented as an ellipsoid of revolution, and on the distance between the poles of the dipole. We refer to the equation he uses to interpret data on amino acids and peptides.[13]
(18) Lifson, S.; Roig, A. *J. Chem. Phys.* **1961**, *34*, 1963.
(19) The $\Delta G°$ values at each ionic strength were calculated for the complete helix from $\Delta G° = -RT \ln (\sigma s^{n-2})$, after determination of the average s value for the peptide from helix–coil theory.[18] A σ value of 0.0029 was used in the calculations along with CD values of −33 750 deg cm² dmol⁻¹ for 100% helix and +640 deg cm² dmol⁻¹ for 0% helix (J. M. Scholtz and R.L.B., unpublished results). Helix–coil theory, together with the determined values of s and σ, indicates that a distribution of partially helical molecules, each with strongly frayed ends, is present. From the values of s and σ, it is nevertheless possible to compute $\Delta G°$ for the complete helix, as indicated. The lines were determined from a linear least-squares fit of the data at high ionic strength ($\Gamma/2 > 1.2$) by imposing a common $\Delta G°$ value at $\Gamma/2 = 0$.[20] The slopes of the lines, K_s, are used to subtract the Hofmeister effect for each salt from the observed $\Delta G°$.
(20) McDevitt, W. F.; Long, F. A. *J. Am. Chem. Soc.* **1952**, *74*, 1773.

Acknowledgment. We thank John Schellman and Hong Qian, University of Oregon, for discussion and for use of their computer program for the Lifson–Roig theory. This research was supported by NIH Grant GM 31475. J. M. Scholtz is an NIH fellow (GM 13451). We thank Leland V. Miller of the NIH Clinical Mass Spectrometry Resource, University of Colorado, supported by Grant RR 01152, for FAB mass spectra and Robert J. Binard for amino acid analysis.

(21) Åqvist, J.; Luecke, H.; Quiocho, F. A.; Warshel, A. *Proc. Natl. Acad. Sci. U.S.A.* **1991**, *88*, 2026.

Template-Directed Interference Footprinting of Protein–Guanine Contacts in DNA

Kathleen C. Hayashibara and Gregory L. Verdine*

Department of Chemistry, Harvard University Cambridge, Massachusetts 02138

Received January 18, 1991

Matched contacts between amino acid residues and DNA bases are important for sequence discrimination by DNA binding proteins.[1] DNA base contacts are thus the subject of chemical methods that probe molecular recognition in protein-DNA complexes.[2-4] These *interference footprinting* methods involve treating DNA with reagents that produce lesions, which are then assayed site-specifically for interference of protein binding; interfering sites are interpreted as contact bases and *vice versa*. Current methods are limited by a common problem: the difficulty of carrying out selective chemical modification of DNA to produce defined lesions that do not significantly alter secondary structure. We report an alternative approach—template-directed interference (TDI) footprinting—that achieves these objectives by enzymatically incorporating base analogues into DNA. Below, we demonstrate the use of TDI footprinting in the analysis of contacts between the *434* repressor protein and guanine (G) residues of the *434* O_R1 operator (binding site).[5]

For TDI footprinting of guanine (TDI-G footprinting), we chose the analogue N^7-methyl-2′-deoxyguanosine (**1**, Scheme I),[6] in which the N^7-methyl group is the interfering function.[2] A radiolabeled primer, annealed to single-stranded DNA[7] containing O_R1, was extended enzymatically by using the four natural 2′-deoxynucleoside 5′-triphosphates (dNTPs) plus the 5′-triphosphate of **1** (1TP) in an amount sufficient to afford approximately one random incorporation per extension.[9] The resulting ensemble of G-methylated DNA molecules was incubated with *434* repressor[10] over a range of protein concentrations,[11] and the protein-bound DNA molecules were separated electrophoretically from unbound DNA.[12] The DNA samples were recovered,

Scheme I

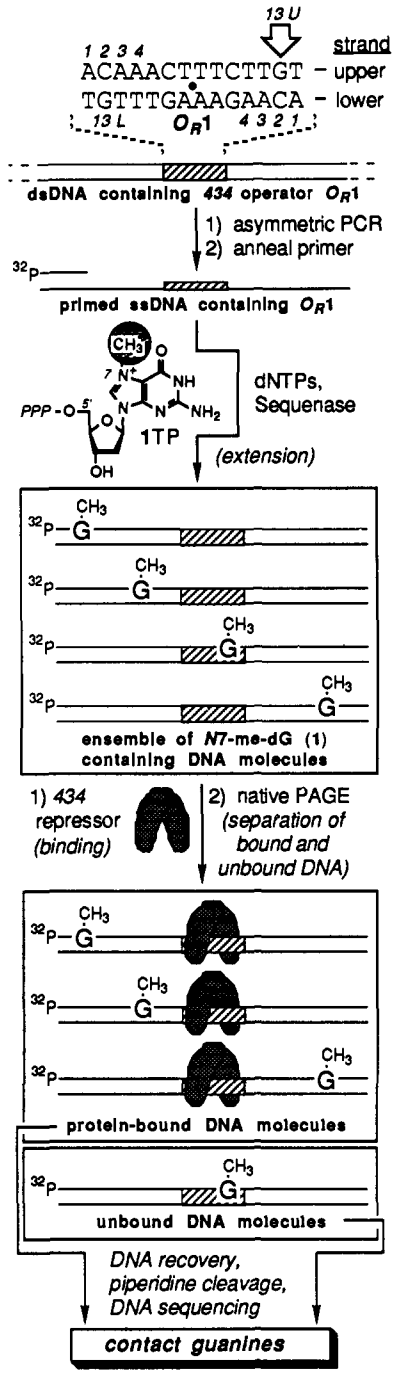

cleaved at residues **1** with piperidine,[2] and electrophoresed on a DNA sequencing gel.[9]

Contact analysis of the O_R1 upper strand (cf. Scheme I) is presented in Figure 1. Sanger sequencing[13] lanes define the O_R1 region, as indicated. The bands in the TDI-G footprint lane *Cn* reveal all sites at which analogue **1** was incorporated; its 1:1 correspondence with the Sanger G-lane demonstrates that the analogue base-pairs only as G. In contrast to the clean DNA modification effected by incorporation of **1**, alkylation of DNA by dimethyl sulfate (DMS lane) produces numerous cleavable

* To whom correspondence should be addressed.

(1) Steitz, T. A. *Q. Rev. Biophys.* **1990**, *23*, 205.
(2) Siebenlist, U.; Gilbert, W. *Proc. Natl. Acad. Sci. U.S.A.* **1980**, *77*, 122.
(3) Brunelle, A.; Schleif, R. F. *Proc. Natl. Acad. Sci. U.S.A.* **1987**, *84*, 6673. Hayes, J. J.; Tullius, T. D. *Biochemistry* **1989**, *28*, 9521.
(4) Nielsen, P. E. *J. Mol. Recognit.* **1990**, *3*, 1.
(5) Aggarwal, A. K.; Rodgers, D. W.; Drottar, M.; Ptashne, M.; Harrison, S. C. *Nature* **1988**, *242*, 899.
(6) Hendler, S.; Fürer, E.; Srinivasan, P. R. *Biochemistry* **1970**, *9*, 4141. Commercially available from Sigma.
(7) The 233 base pair (bp) template DNA was obtained by asymmetric PCR (APCR)[8] using a plasmid donor having O_R1 cloned into the polylinker.[9]
(8) Gyllensten, U. B.; Erlich, H. A. *Proc. Natl. Acad. Sci. U.S.A.* **1988**, *85*, 7652.
(9) Detailed experimental descriptions are deposited in the supplementary material or may be obtained directly from the authors by FAX (617-495-8755).
(10) Koudelka, G. B.; Harrison, S. C.; Ptashne, M. *Nature* **1987**, *326*, 886.
(11) Concentration variation allows one in principle to distinguish the effect of modifying each guanine on the K_d of the protein–DNA complex.
(12) Chodish, L. A. In *Current Protocols in Molecular Biology*; Ausubel, F. M., Brent, R., Kingston, R. E., Moore, D. D., Smith, J. A., Seidman, J. G., Struhl, K., Eds.; John Wiley & Sons: New York, 1989; Vol. 2, pp 12.2.1–12.2.10.
(13) Sanger sequencing was carried out by using the same ^{32}P end labeled, primed ssDNA used in TDI-G footprinting (Scheme I). Sanger, F.; Nicklen, S.; Coulson, A. R. *Proc. Natl. Acad. Sci. U.S.A.* **1977**, *74*, 5463.

0002-7863/91/1513-5104$02.50/0